

Galactic dark matter search via phenomenological astrophysics modeling

Xiaoyuan Huang,¹ Torsten Enßlin,^{2,3,4} Marco Selig^{2,5}

¹Physik-Department T30d, Technische Universität München, James-Franck-Straße, D-85748 Garching, Germany

²Max-Planck-Institut für Astrophysik, Karl-Schwarzschildstraße 1, D-85748 Garching, Germany

³Ludwig-Maximilians-Universität München, Geschwister-Scholl-Platz 1, D-80539 Munich, Germany

⁴Exzellenzcluster Universe, Technische Universität München, Boltzmannstr. 2, D-85748 Garching, Germany

⁵IBM R&D GmbH, Schönaicher Straße 220, D-71032 Böblingen, Germany

E-mail: xiaoyuan.huang@tum.de, ensslin@mpa-garching.mpg.de, mseelig@mpa-garching.mpg.de

Abstract. Previous searches for the γ -ray signatures of annihilating galactic dark matter used predefined spatial templates to describe the background of γ -ray emission from astrophysical processes like cosmic ray interactions. In this work, we aim to establish an alternative approach, in which the astrophysical components are identified solely by their spectral and morphological properties. To this end, we adopt the recent reconstruction of the diffuse γ -ray sky from Fermi data by the D³PO algorithm and the fact that more than 90% of its flux can be represented by only two spectral components, resulting from the dense and dilute interstellar medium. Under these presumptions, we confirm the reported DM annihilation-like signal in the inner Galaxy and derive upper limits for dark matter annihilation cross sections. We investigate whether the DM signal could be a residual of the simplified modeling of astrophysical emission by inspecting the morphology of the regions, which favor a dark matter component. The central galactic region favors strongest for such a component with the expected spherically symmetric and radially declining profile. However, astrophysical structures, in particular sky regions which seem to host most of the dilute interstellar medium, obviously would benefit from a DM annihilation-like component as well. Although these regions do not drive the fit, they warn that a more detailed understanding of astrophysical γ -ray emitting processes in the galactic center region are necessary before definite claims about a DM annihilation signal can be made. The regions off the Galactic plane actually disfavor the best fit DM annihilation cross section from the inner Galactic region unless the radial decline of the Galactic DM density profile in the outer regions is significantly steeper than that usually assumed.

Contents

1	Introduction	1
2	The Gamma-ray sky	2
2.1	The astrophysical gamma ray sky	2
2.2	DM annihilation	4
2.3	The likelihood	4
3	Results	5
3.1	Pure astrophysics	5
3.2	DM annihilation	6
3.3	Upper limits	10
3.4	Extragalactic component	11
4	Conclusions	12

1 Introduction

The presence and therefore the existence of dark matter (DM) in the Universe has been confirmed through many independent astrophysical studies, while the physical nature of DM particles is still unknown [1–4]. A promising way to probe the nature of DM is to identify its annihilation signatures. In many scenarios, DM particles froze-out in the primordial Universe, and this kind of thermal production promises a non-negligible annihilation cross section. The dense centers of galaxies and galaxy clusters should therefore be sites of DM annihilation events. The thereby produced charged particles and photons might be detectable and thereby reveal particle properties of DM [5–11]. Unlike any charged particle created by DM annihilation, which loses its directional information during its propagation, annihilation γ -rays should provide precise information on the spatial distribution of DM as well as direct hints on the mass of DM particles in some extreme cases [12–17]. Sky locations such as dwarf galaxies, galaxy clusters and the Galactic center, which are promising for indirect detection of DM using γ -ray data, should contain DM in high density, be relatively nearby, and show little flux of astrophysical (not-DM-annihilation related) γ -rays. The GC region is ideal with respect to the first two conditions, however, it exhibits unfortunately significant astrophysical γ -ray sources as it harbors supernovae explosions injecting cosmic rays (CRs) into the interstellar medium (ISM) and compact sources of high energy particles and radiation [18].

Several groups have analyzed the publicly-available Fermi-LAT data and reported a spatially extended γ -ray excess of around 1 – 3 GeV from the region surrounding the Galactic Center (GC) with respect to the expected diffuse Galactic γ -ray emission (DGE) of astrophysical, non-DM origin [19–27]. In general, it was found that dark matter with several tens of GeV, which annihilates into $b\bar{b}$ and $\tau^-\tau^+$ final states, would account for the spectral shape [28, 29] and a generalized NFW profile [30, 31] with an inner slope $\alpha = 1.2$ would explain the spatial extension of this excess [26–28].

The DGE model assumed in these works was usually that of the Fermi collaboration. This model is constructed by assuming the flux to be described by a linear superposition

of spatial templates, which are partly directly observations at other wavelength, partly the result of physical modeling of the CR propagation and interaction in the Galaxy.

It is anticipated that the DGE model uncertainties affect the apparent GeV γ -ray excess towards the GC, which implies considerable systematic uncertainties for the deduced DM properties or upper limits. Zhou et al. [32] and Calore et al. [28] address this by scanning the model parameter space by changing the simulated CR source distributions, CR propagation parameters, and CR target properties. The presence of the GeV excess signal seems to be robust with respect to the resulting changes in the DGE template, however, the spectral shape of the GeV excess seems to vary to some degree.

In addition to their investigation of theoretical uncertainties of the different DGE models, Calore et al. [28] performed a principal component analysis of the γ -ray flux residuals in a number of test regions along the Galactic plane which permitted them to estimate empirically their model uncertainties. The best fit DM parameters derived in this careful investigation will be compared to the results presented from our analysis.

Apart from DM annihilation, γ -ray emission from millisecond pulsars could also be the origin of the GeV excess. Millisecond pulsars are believed to be abundant in the GC and their spectra also peak at several GeV. A blend of unresolved millisecond pulsars should appear as extended γ -ray emission to the Fermi-LAT instrument [23, 24, 33–35]. However no millisecond pulsar has yet been identified in the GC region. This non-detection questions the millisecond pulsar scenario [36, 37] unless their brightness distribution function resides mostly below the sensitivity of Fermi-LAT [38]. Recent investigations [39, 40] show that unresolved point sources could indeed account for the GeV excess.

The unclear picture drawn by these studies motivates us to scrutinize the reported potential DM annihilation signal for the possibility that the reported γ -ray excess is due to imperfections in the DGE and point source modeling. To this end, an alternative, template-free, non-parametric, and phenomenological DGE and point source model, which significantly differs from that of the Fermi collaboration and other groups, is used in the following search for a Galactic γ -ray DM signal.

2 The Gamma-ray sky

2.1 The astrophysical gamma ray sky

Our DGE model is based on the recent re-analysis of the Fermi γ -ray data in terms of diffuse flux and point sources by Selig et al. [41]. Selig et al. [41] used the D³PO algorithm [42] to produce noise- and point source-cleaned maps of the diffuse γ -ray emission at nine logarithmically spaced energy bands ranging from just below 1 GeV to 300 GeV.

D³PO stands for “Denoising, deconvolving, and decomposing photon observations” and is an imaging algorithms for high energy photons. D³PO assumes the γ -ray sky to be composed of a diffuse component, which varies on a logarithmic scale but exhibits spatial correlations, and a point-source component, which consists of spatially uncorrelated point sources with a power-law brightness distribution. Using this, D³PO decomposes the observed photon flux into these components probabilistically while also taking the instrument response and the Poisson statistics of the γ -ray events into account. The D³PO algorithm is derived in the context of information field theory [43], the information theory for fields, and implemented using the numerical information field theory (NIFTY) library [44], which permits the construction of space-pixelization independent code. In consequence, D³PO provides two sky maps, one containing the diffuse emission component and one the point source component,

the latter having virtually a source in each pixel, however, most of them being infinitesimally weak.

In contrast, astrophysical gamma ray model based on the Fermi Collaboration data products account only for the presence of the point sources which were detected above the significance threshold chosen by the Fermi Collaboration. This permits the possibility that dense sub-threshold sources appear as an extended source, distinct from the astrophysical γ -ray model, which might mimic DM annihilation.

In contrast to this, the analysis by Selig et al. [41] takes marginally detected point sources into account probabilistically. Only populations of even weaker, individually unresolved point sources would be missed by D³PO as well. Whether such sources could account for the GeV excess is an open question [39, 40].

An important observation of Selig et al. [41] was that more than 90% of the DGE at all sky locations and all investigated energies could be accounted for by a simple, phenomenologically constructed two component model: The γ -ray spectra of a molecular cloud complex in the Galactic anti-center and that of the southern tip of the southern Fermi bubble [45–47] served as spectral templates in a point-to-point spectral fitting of the nine D³PO maps at different energies. The result of this analysis showed “cloud-like” gamma-ray emission with a spatial morphology closely resembling that of Galactic dust maps derived from completely independent microwave [48] or far-infrared [49] observations. This, as well as the steep spectrum with a hint of a bump at GeV as typical for γ -rays from the decay of π^0 s indicates that the “cloud-like” component is mostly due to hadronic CR proton interactions in the denser parts of the ISM [41]. The “bubble-like” component showed prominently the Fermi-bubbles, as well as an puffed up version of the Galactic disc. This morphology, as well as the harder, power-law like spectrum indicates that this component is mostly due to inverse Compton up-scattering of photons by CR electrons, which predominantly occurs in the volume-dominating hot and dilute part of the ISM [41]. The Fermi bubbles are then just two giant outflows driven by the hot ISM and in particular the light CR content of it, as a number of authors already suggested [46, 50].

The association of the two radiation processes to the two ISM phases is certainly not unique, as each of them will happen in each phase, but the preferences are certainly correct due to the very different nuclear target densities.

Since the phenomenological two component description of the DGE successfully captures the dominant γ -ray properties of the Milky Way, we will assume it to be correct within this work. As both used spectral templates were taken from regions far from the GC, they should be little contaminated by γ -rays from potential DM annihilation or other processes only predominantly occurring in the GC. Any such contribution should – if it does not mimic our spectral templates – be visible in terms of excess γ -rays with respect to our two component model. In the following we will test the data for such excess photons.

Our phenomenological two component DGE model can certainly be criticized for its simplicity, the neglect of spectral differentiating CR transport processes, and its ignorance to the existing detailed knowledge on radiation processes. It is meant as an orthogonal approach to the existing DM searches, which should show which aspects of these investigations are robust, and which might need improvements. We believe that an unmatched strength of our approach is the flexible, non-parametric form of the spatial template generation. In the approaches so far, the used, more rigid spatial templates could potentially be inadequate to represent the real DGE.

Our spectral resolution will be limited to the energy bin choice of Selig et al. [41].

Although a higher spectral resolution than nine energy bands in the range of $\sim 1 \dots 300$ GeV would certainly be desirable, this is not feasible. The current version of the D³PO algorithm has to process individual bands separately and requires that each band has a sufficiently high photon statistics to perform a good decomposition of the sky into point sources and diffuse flux. As shown below, our analysis reproduces well the reported GC γ -ray excess and finds very similar DM parameters as reported in Calore et al. [28]. This indicates that the limited spectral resolution of our analysis does not hamper our sensitivity for DM annihilation.

2.2 DM annihilation

Following previous work [26–28], we model the radial distribution of Galactic DM

$$\rho(r) = \frac{\rho_s}{(r/r_s)^\alpha (1 + r/r_s)^{3-\alpha}} \quad (2.1)$$

as a generalized NFW profile [30, 31] with an inner slope of $\alpha = 1.2$. We determine the normalization ρ_s by fixing the DM density at the solar radius to $\rho(r_\odot = 8.5 \text{ kpc}) = 0.4 \text{ GeV cm}^{-3}$ [51–53].

We investigate the DM parameter space spanned by the DM mass m_{dm} and velocity-averaged cross sections $\langle\sigma v\rangle$. We scan through this parameter plane in a logarithmically equal spaced grid with m_{dm} taking twenty values between $5 \text{ GeV}/c^2$ and $200 \text{ GeV}/c^2$ as well as $\langle\sigma v\rangle$ taking fifty values in between 10^{-5} to 5 in unit of $3 \times 10^{-26} \text{ cm}^3\text{s}^{-1}$. As in previous works, we investigate the most common annihilation final states $b\bar{b}$ and $\tau^-\tau^+$, and we use the corresponding spectrum derived from PPPC4DMID, in which electro-weak corrections are included [54].

2.3 The likelihood

To be consistent with the adopted DGE modeling, we use the same data set as in [41]. The 6.5 years Fermi reprocessed Pass 7 CLEAN data are binned in nine logarithmically spaced energy bands ranging from 0.6 to 307.2 GeV, and the sky is discretized by HEALPix scheme with $n_{side}=128$, which corresponds to an angular resolution of approximately 0.46° . For each energy bin, the data are further split into FRONT and BACK events according to where in the LAT instrument the photons were registered. D³PO has difficulties to accurately model the γ -ray sky in the highest energy bin since the low number of photons there inhibit a clear separation into diffuse and point like flux. For this reason, Selig et al. [41] ignored this bin in any further analysis and we will do so as well. The corresponding Fermi LAT instrument response and exposure functions necessary for the data analysis are generated by Fermi Science Tools¹.

As described above, D³PO could decompose the γ -ray sky into point source components and diffuse component, in which the contribution of possible DM annihilation could be embedded. The “cloud-like” and the “bubble-like” components from Selig et al. [41] are convolved with the energy dependent instrument response and exposure functions yielding the expected number of counts, n_c^{ijk} and n_b^{ijk} respectively, in each pixel i , each energy bin j , and for each photon detection mode k (FRONT or BACK). The combined index ijk fully indexes our data space here and in all following formula.

This model of expected counts is however constructed without taking the presence of a third component, annihilating DM, into account. In order to fix this and to release DM

¹<http://fermi.gsfc.nasa.gov/ssc/data/analysis/software/>

annihilation flux potentially absorbed by the DGE components, their spatial morphology is made flexible here. To this end, two free fitting parameters α_i and β_i are introduced for each spatial pixel i , such that $n_c^{ijk} \rightarrow \alpha_i n_c^{ijk}$ and $n_b^{ijk} \rightarrow \beta_i n_b^{ijk}$.

For fixed DM properties, such as the annihilation final states, m_{dm} , and $\langle\sigma v\rangle$, the expected number n_{dm}^{ijk} of DM induced γ -ray counts for all data space locations ijk can be calculated. These, plus the corresponding expected photon counts due to the ‘‘cloud-like’’ γ -ray emission, $\alpha_i n_c^{ijk}$, the ‘‘bubble-like’’ γ -ray emission, $\beta_i n_b^{ijk}$, and the point sources, n_{point}^{ijk} , form the total expected γ -ray counts

$$\lambda^{ijk} = n_{\text{dm}}^{ijk} + \alpha_i n_c^{ijk} + \beta_i n_b^{ijk} + n_{\text{point}}^{ijk}. \quad (2.2)$$

The expected γ -ray counts λ^{ijk} depend on the assumed DM model (m_{dm} and $\langle\sigma v\rangle$) and set of fitting parameters ($\alpha = (\alpha_i)_i$, $\beta = (\beta_i)_i$), collectively called the parameters $p = (m_{\text{dm}}, \langle\sigma v\rangle, \alpha, \beta)$. These expected counts should be compared to the actually observed number of photons n_{obs}^{ijk} to infer these parameters p . We do this by minimizing the objective functions given by the negative log-likelihood

$$\begin{aligned} \chi_{\text{ROI}}^2(p) &\equiv \sum_{i \in \text{ROI}} \chi_i^2(p) \text{ with} \\ \chi_i^2(p) &\equiv -2 \ln L_i(d_i|p) \end{aligned} \quad (2.3)$$

for any special region of interest (ROI) pixel-wise with respect to α_i and β_i , the re-normalizations of the ‘‘cloud-like’’ and ‘‘bubble-like’’ γ -ray emission, while scanning through the DM parameter subspace. Here, the data vector $d_i = \left(n_{\text{obs}}^{ijk}\right)_{jk}$ of the counts associated with pixel i is introduced as well as the the pixel-wise Poisson count likelihood $L_i(d_i|p)$, by

$$\ln L_i(d_i|p) = \sum_{jk} \left[n_{\text{obs}}^{ijk} \ln \lambda^{ijk} - \lambda^{ijk} - \ln \left(n_{\text{obs}}^{ijk}! \right) \right]. \quad (2.4)$$

The last term in the brackets has no influence on the fit and is therefore ignored in the analysis.

The DM distribution is concentrated towards the center of the Milky Way, which is, unfortunately, one of the most complicated sky area due to the various astrophysical sources there. To become insensitive to our probably imperfect modeling of the central Galactic region, we define ROIs which exclude it from our analysis. Furthermore, since numerous faint, undetected and therefore not-modeled point sources may reside in the Galactic plane, which nevertheless might contaminate the diffuse emission, we also mask the Galactic plane for these ROIs to ensure the validity of our two components astrophysical diffuse model. As our primary ROI we select Galactic latitudes $4^\circ < |b| < 20^\circ$ and Galactic longitudes $|l| < 20^\circ$ similar to the ROI used in [28], but masking a bit more of the Galactic plane region. For comparison, we select also a test ROI, which excludes any area close to the GC and close to the galactic plane. For the test ROI we expect the contribution of DM annihilation to the γ -ray sky to be negligible. These ROIs are shown in Fig. 1.

3 Results

3.1 Pure astrophysics

First, we investigate the possibility for a purely astrophysical γ -ray sky without DM annihilation signatures, which means to set $n_{\text{dm}}^{ijk} = 0$ while fitting the remaining model parameters

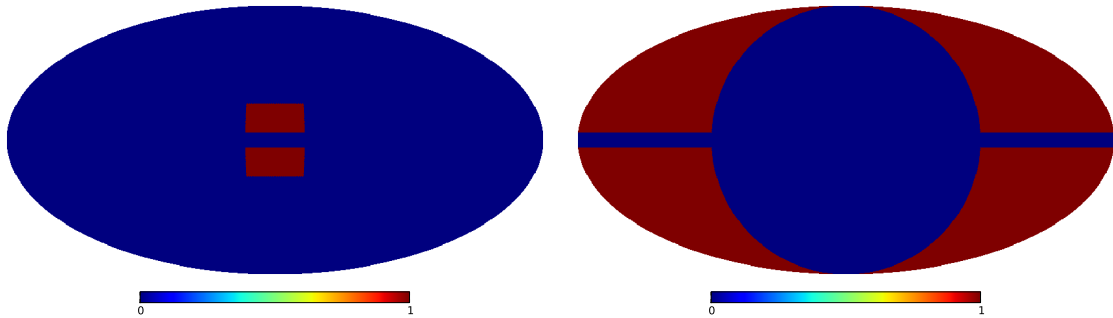


Figure 1. Regions used in our analysis. The primary ROI is left and the test ROI is right.

α and β for all locations $i \in \text{ROI}$. Fig. 2 shows the observed and modeled counts within the two ROIs described above as well as the residuals between model and data. In both ROIs, a purely astrophysical DGE model fits the data reasonably well. The largest residual appears in the highest used energy bin. There, the limited photon statistics might still cause problems to D³PO in separating point sources from diffuse emission as it clearly has done at the next higher energy bin. Therefore, we do not consider the discrepancy between model and data at this energy as an serious indicator of DM or other new physics. However, a small, but significant photon count excess around several GeV can be recognized as well for our primary ROI, but not for the test ROI. This excess seems to be the GeV excess reported in the literature and might be a possible DM annihilation signature.

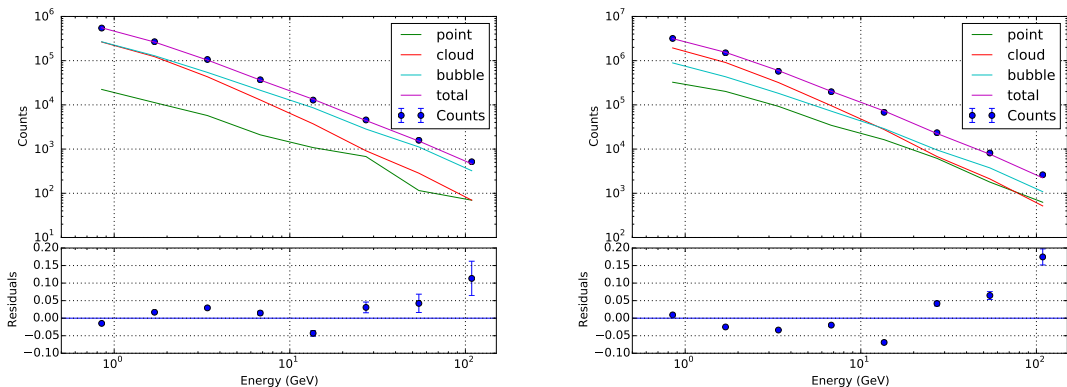


Figure 2. Photon counts and relative residuals for a purely astrophysical sky model within our primary ROI (left) and test ROI (right). Here, cloud and bubble refer to the emission components with cloud-like and bubble-like spectra identified in [41], respectively.

3.2 DM annihilation

To investigate whether the GeV photon count excess observed within our primary ROI could be caused by DM annihilation, we scan dark the matter parameters m_{dm} and $\langle\sigma v\rangle$ while fitting the astrophysical DGE parameter sets α and β . The corresponding improvement of

our objective function

$$\delta\chi_{\text{ROI}}^2(m_{\text{dm}}, \langle\sigma v\rangle) = \min_{\alpha,\beta}\chi_{\text{ROI}}^2(0, 0, \alpha, \beta) - \min_{\alpha,\beta}\chi_{\text{ROI}}^2(m_{\text{dm}}, \langle\sigma v\rangle, \alpha, \beta) \quad (3.1)$$

thanks to the presence of DM is shown in Fig. 3 for the $b\bar{b}$ and $\tau^-\tau^+$ final state DM annihilation chains. Within this we also identify the best fit DM parameters $(m_{\text{dm}}, \langle\sigma v\rangle)_*$ with maximum $\delta\chi_{\text{ROI}}^2$. These best fit locations agree well with the ones found by Calore et al. [28], who consider DGE model uncertainties and also empirical model systematics in their analysis. As a sanity check, one can verify that the resulting cloud-like and bubble-like components (Fig. 4) do not seem obviously be disturbed by the presence of DM annihilation. For instance, there is no evident emission decrement at the GC apparent on these maps. Had there been one, it would have been an indication of the DM component fitting away the astrophysical ones.

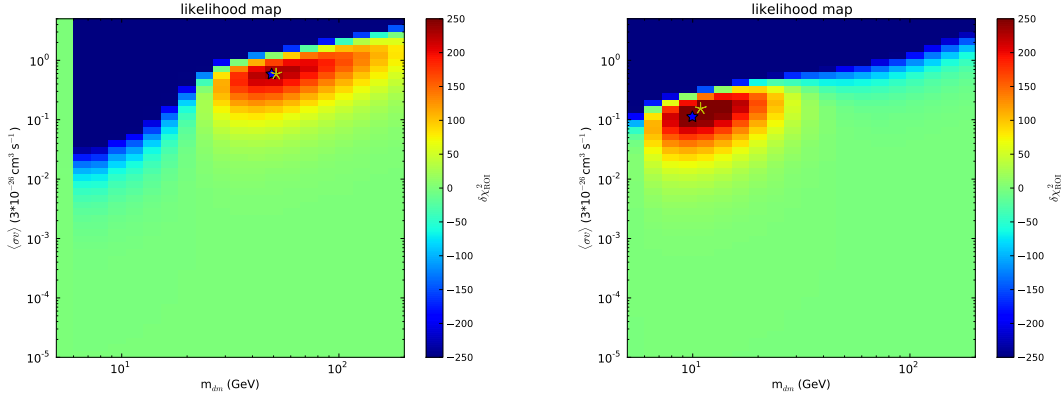


Figure 3. The likelihood for $b\bar{b}$ (left) and for $\tau^-\tau^+$ (right) final annihilation states in terms of $\delta\chi_{\text{ROI}}^2(m_{\text{dm}}, \langle\sigma v\rangle)$ given by Eq. 3.1 for the primary ROI. The blue stars indicate best fit values from [28] and the yellow stars are our best fit DM parameters $(m_{\text{dm}}, \langle\sigma v\rangle)_*$.

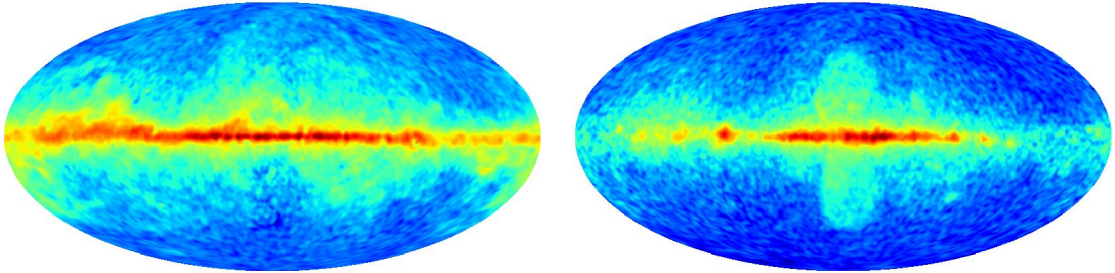


Figure 4. Cloud-like (left) and bubble-like (right) gamma-ray emission components in logarithmic units after permitting for the presence of DM annihilation for the best fit DM model with the $b\bar{b}$ annihilation channel.

As a further check, we change the ROIs to verify that the best fit DM parameters $(m_{\text{dm}}, \langle\sigma v\rangle)_*$ inferred from different regions are consistent with each other. We choose three regions with different angular distances to the GC: from 0 to 10 degrees, 10 to 15 degrees and 15 to 20 degrees, and in each region we also mask out the inner 4 degrees of the galactic disk in latitude, see Fig. 5. The corresponding likelihood maps for $b\bar{b}$ annihilation final states (also Fig. 5) are consistent with each other and exhibit only slightly changing best fit DM parameters $(m_{\text{dm}}, \langle\sigma v\rangle)_*$.

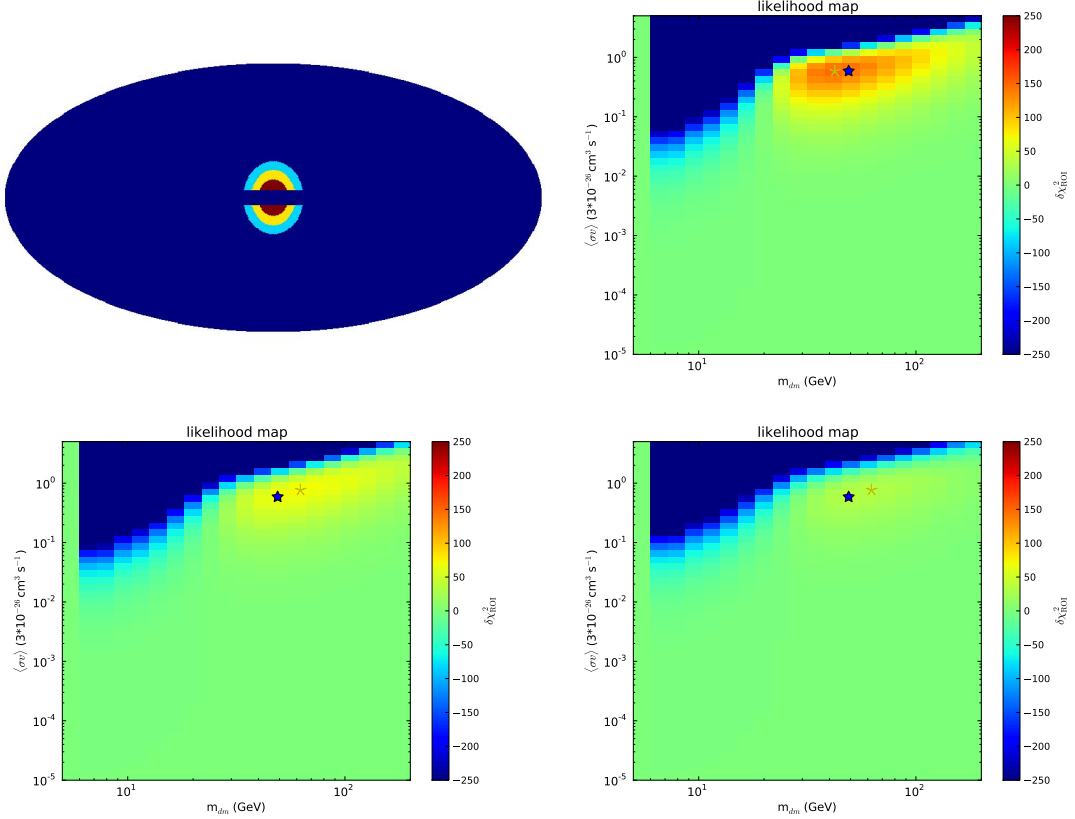


Figure 5. Top left: Different ROIs to test the consistency of the best fit DM parameters $(m_{\text{dm}}, \langle\sigma v\rangle)_*$. Top right to bottom right: Corresponding $\delta\chi_{\text{ROI}}^2(m_{\text{dm}}, \langle\sigma v\rangle)$ given by Eq. 3.1 for $b\bar{b}$ final annihilation states for these ROIs from inside out. Here the blue stars indicate best fit values from [28] and the yellow stars are our best fit DM parameters for the corresponding ROIs.

In order to test for a potential astrophysical, non-DM annihilation related origin of this signal we try to identify the sky locations driving $\delta\chi_{\text{ROI}}^2$. To this end we construct all sky maps of $\delta\chi_*^2$ for the best fit DM parameters $(m_{\text{dm}*}, \langle\sigma v\rangle_*)$ as

$$\delta\chi_{*i}^2 = \min_{\alpha_i, \beta_i} \chi_i^2(0, 0, \alpha_i, \beta_i) - \min_{\alpha_i, \beta_i} \chi_i^2(m_{\text{dm}*}, \langle\sigma v\rangle_*, \alpha_i, \beta_i). \quad (3.2)$$

In case such a map exhibits the morphology of a known galactic structure, like the Fermi bubbles, the molecular clouds, or others, this structure will be suspected to be the origin of an only apparent DM signal. Fig. 6 shows that the improvement in χ^2 due to the inclusion of DM annihilation γ -rays is almost spherically distributed around the GC. This χ^2 improvement is also seen at the regions around GC, which were excluded from the fit. This

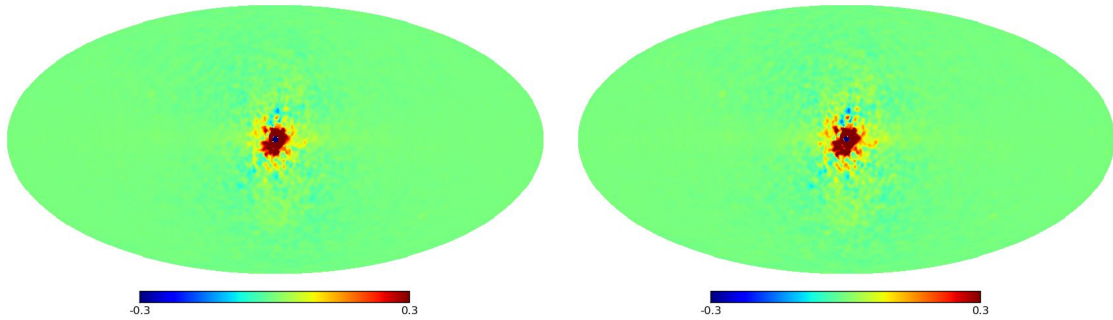


Figure 6. The map of the likelihood improvements $\delta\chi_{\star i}^2$ due to a DM components with properties $(m_{\text{dm}}, \langle\sigma v\rangle)_{\star}$ according to Eq. 3.2 for $b\bar{b}$ (left) and $\tau^-\tau^+$ (right) final annihilation states.

is as it should be in case this radiation was a missing element of the γ -ray sky. The pixels at the very center of the Galaxy do not request a DM component. However, the strong CR accelerators there with different spectra compared to our simplistic DGE components might have confused the fit.

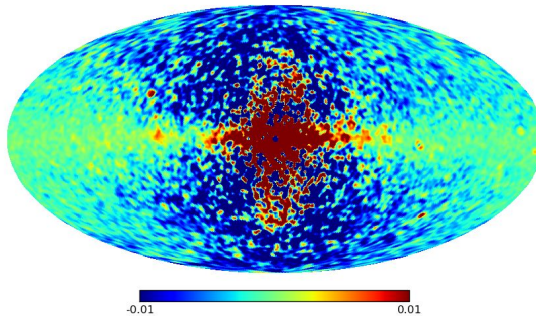


Figure 7. Like left panel of Fig. 6, but with rescaled and strongly saturated color scale to highlight non-central regions.

Anyhow, an inspection of the more subtle χ^2 -changes made visible by tuning the colorbar (Fig. 7) reveals the morphology of the Fermi bubbles as well as of the galactic disk in $\delta\chi_{\star i}^2$ structures at locations more distant from the GC. This suggests a single “bubble-like” spectra to be an imperfect representation of the hot ISM γ -emission spectrum and that existing variations therein have spectral similarity with the spectrum of DM annihilation. The contribution of these morphologically suspect regions to the total $\delta\chi_{\text{ROI}}^2$ is marginal, but could indicate a problem also prevailing within our primary ROI.

A spectral component resembling DM annihilation improves the fit also at locations where not much DM annihilation is expected. In order to investigate this a bit further, the following experiment is performed: The spatial DM template is allowed change by introducing modification factors γ_i via the replacement $n_{\text{dm}}^{ijk} \rightarrow \gamma_i n_{\text{dm}}^{ijk}$ in Eq. 2.2. Fig. 8 compares the original n_{dm}^i -map with the $\gamma_i n_{\text{dm}}^i$ -map resulting from a simultaneous fit in α , β , and γ with the DM parameters are fixed to $(m_{\text{dm}}, \langle\sigma v\rangle)_{\star}$ and assuming $b\bar{b}$ annihilation final states. A

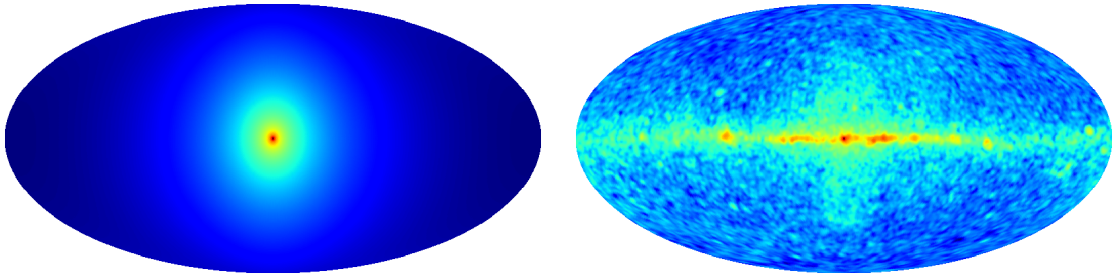


Figure 8. In the left panel we show the anticipated spatial distribution of the number of counts n_{DM}^i from DM annihilation, and in the right panel we show $\gamma_i n_{\text{DM}}^i$, which indicate the spatial distribution of number of counts from fitting with new parameter γ_i .

numerical comparison of the Galactic inner regions of these maps shows that the spatial DM template is relatively good, as the modification factors have values around unity in there, which is consistent with the result in Fig. 3.

However, Fig. 8 also shows that a spectral component mimicking DM annihilation is strongly wanted by the data for regions without much expected DM signal. In particular, regions hosting the hot interstellar medium seem to request such a DM-like spectral component (compare to Fig. 4). This kind of possible bipolar structures is also favored in recent work [55, 56] for the morphology of GeV excess. This is, on the one hand, an indicator that our simplistic two component galactic model is not complex enough to fully represent the inverse Compton emission of the Galaxy. Given the short cooling times of the relativistic electrons involved in this channel, some spectral variations in their emission is not too surprising. On the other hand, the preferred dilute ISM-like morphology of a DM-like spectral component disfavors the DM annihilation scenario as well as the possibility of a blend of weak γ -ray emitting point sources for their expected very different γ -ray morphologies.

Previously proposed astrophysical explanations, such as extra CR in the GC producing leptons [57–59] could possibly contribute to the bubble shape structures, and a population of Galactic millisecond pulsars [23, 24, 33–37, 39, 40] could in principle also contribute to the γ -ray emission Galactic disk.

3.3 Upper limits

Large DM annihilation cross sections can be excluded, as they would imply γ -ray counts strongly in excess to the data. Here, we switch back to assuming the DM to have spatially a generalized NFW profile. Upper limits on $\langle\sigma v\rangle$ should be placed (as a function of DM mass m_{dm} and final state channel of the annihilation) at the transition from green to blue in Fig. 3 and Fig. 9 for the primary and test ROI, respectively.²

It is interesting to note that the test ROI seems to be far more exclusive for DM models compared to previous work deriving upper limits from high latitude region [60–63], if we ignore the DM-affine region in the parameter space for $b\bar{b}$ visible in Fig. 9, which is driven by an excess in the lowest energy bin only (see Fig. 2). These exclusion limits are so high that they seem to exclude the best fit scenarios for our primary ROI. These limits, however,

²Specifying a formal statistical upper limit curve would pretend a not justified precision since this work shows that the DGE model systematics dominate the uncertainty budget.

depend strongly on the validity of the adopted NFW profile in the outer Galaxy, which certainly can be questioned.

To investigate the robustness of the exclusion limit on the assumed DM profile we generalize the NFW profile to

$$\rho(r) = \frac{\rho_s}{(r/r_s)^\alpha (1 + r/r_s)^{3-\alpha+\gamma}}. \quad (3.3)$$

Here, we keep $\alpha = 1.2$ to accommodate the GeV excess in the inner Galaxy region, but add the parameter γ to describe a possible deviation of the DM profile from NFW in the outer regions of the Galaxy. Since we determine the normalization ρ_s by fixing the DM density at the solar radius to $\rho(r_\odot = 8.5 \text{ kpc}) = 0.4 \text{ GeV cm}^{-3}$ [51–53] with fixed $r_s = 20 \text{ kpc}$, ρ_s changes slightly according to the choice of γ . We repeat our analysis for DM profiles with $\gamma = 0.0, 0.5, 1.0, 1.5$ and 2.0 in both, the primary and test ROIs. The resulting best fit DM parameters of the primary ROI and the upper limits from the test ROI are shown in Fig. 10. With increasing γ the best fit cross section derived within the primary ROI decreases due to the mentioned change in the DM normalization. Simultaneously, the upper limits derived within the test ROI increases due to the reduced DM density in the outer Galaxy region. For the here chosen threshold of $\Delta\chi^2 = -100$ a value of $\gamma \geq 1,5$ is required to make the test ROI upper limits consistent with the primary ROI best fit parameters for both, $b\bar{b}$ and $\tau^-\tau^+$ annihilation final states.

Anyhow, the fact that the galactic disk desires a DM-like γ -ray component, whereas the regions above the disk prefer it to be on a lower level, is again indicative to an astrophysical nature of this component.

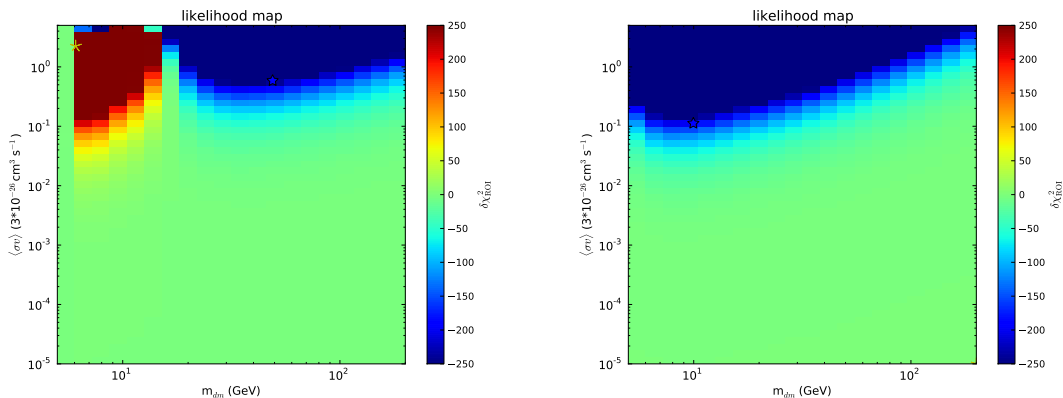


Figure 9. The likelihood for $b\bar{b}$ (left) and for $\tau^-\tau^+$ (right) annihilation final states in terms of $\delta\chi_{\text{ROI}}^2(m_{\text{dm}}, \langle\sigma v\rangle)$ given by Eq. 3.1 for the test ROI. The blue stars indicate best fit values from [28] and the yellow stars are for the test ROI our best fit DM parameters $(m_{\text{dm}}, \langle\sigma v\rangle)_*$.

3.4 Extragalactic component

So far, we assumed that the DGE could be decomposed into only two spectral components, the “cloud-like” and the “bubble-like”. At least an additional extragalactic component exist as well. This has a different spectral form as it is dominated by active galaxies. Its flux distribution can be approximated as being spatially isotropic for our purpose. We investigate how much the results change when we include this extragalactic component into the

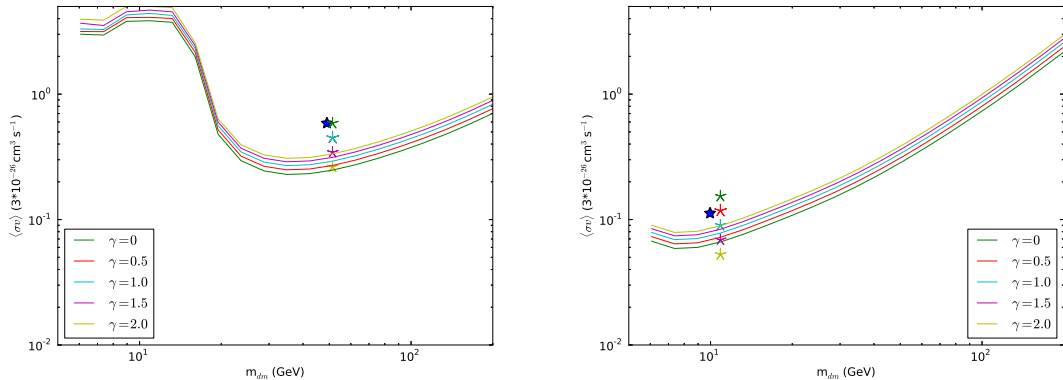


Figure 10. Impact of the assumed Galactic DM profile for different values of γ coded in different colors. The best fit DM parameters derived within the primary ROI (symbols) and upper limits from test ROI (lines) for $b\bar{b}$ (left) and for $\tau^-\tau^+$ (right) annihilation final states are shown. The blue stars are best fit values from [28]. Colored lines are upper limits derived from the test ROI at $\Delta\chi^2 = -100$. The best fit parameters from the primary ROI are marked as stars.

analysis. For this we only investigate the case of the $b\bar{b}$ annihilation final states as an illustrative example. The Fermi Collaboration did a very comprehensive analysis of the isotropic extragalactic emission[64], from which we adopt the spectra of the extragalactic background. This is then converted into expected extragalactic counts n_{iso}^{ijk} as described in Sect. 2.3. The extended model for the total expected counts $\lambda^{ijk} = n_{dm}^{ijk} + \alpha_i n_c^{ijk} + \beta_i n_b^{ijk} + n_{point}^{ijk} + n_{iso}^{ijk}$ is then fitted to the data in the manner described before. In Fig. 11 the resulting spectra of the different components, the likelihood improvement in the DM parameter plane, as well as on the sky is shown for the primary ROI. The inclusion of this additional component does not significantly change our results.

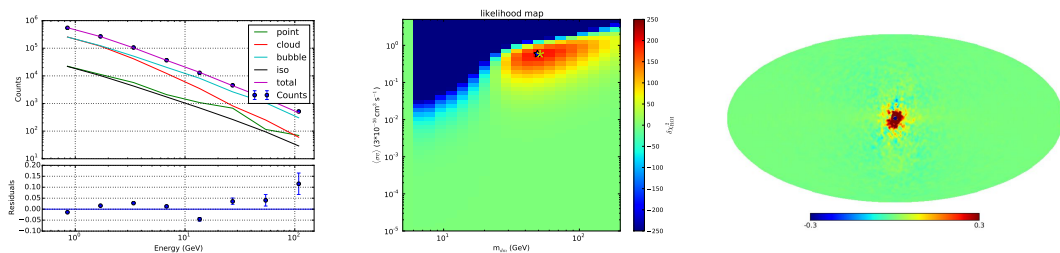


Figure 11. In the left panel we show the spectral shape of different astrophysical diffuse components after considering the isotropic emission. In the middle panel we show the likelihood map as in Fig. 3, and in the right panel we show the pixel by pixel ts map as in Fig. 6.

4 Conclusions

We confirm the presence of the reported apparent GC DM annihilation signal. In contrast to previous studies, we use a phenomenological model for the astrophysical (non-DM related) γ -ray sky, which does not assume any spatial template and for which the spectral templates of the astrophysical components were derived directly from the γ -ray data. To this end, we

adopted the “cloud-like”, “bubble-like”, and point source components of the Fermi-LAT data analysis by Selig et al. [41], added DM annihilation flux for various DM scenarios resulting from a NFW profile and permitted the “cloud-like” and “bubble-like” components to change their morphology to accommodate the latter. Our best fit DM parameters are very similar to those of previous studies, while using a different model for the astrophysical (non-DM related) γ -ray sky. That our independent and methodologically orthogonal modeling of the DGE confirms former findings should increase the confidence in the existence of a GC γ -ray excess, potentially originating from DM annihilation.

In order to investigate whether the potential DM signal is not mimicked by a third astrophysical component, we visualized the forces acting on the likelihood and permitted for free morphologies of the DM annihilation signal distributions. These tests show that the data strives for a DM component centered on the GC, as it would be expected. However, we find that a DM-annihilation like spectral and spatial component improves the fit also at locations hosting predominantly astrophysical γ -ray sources, in particular regions hosting the hot interstellar medium. Furthermore, regions well above the disk, which are relatively free from γ -ray emission, are in tension with a DM-signal of the strength suggested by the GC region. Unless the spatial DM distribution of the Milky Way is much less extended than described by the adopted NFW profile, the DM annihilation interpretation of the excess flux is disfavored by the data.

These observations should be taken as a warning, indicating that also our two component DGE model is not sufficient to capture the full complexity of the astrophysical γ -ray sky. A third astrophysical component seems plausible, which is potentially mimicking the GC DM-signature, but is also present in the Galactic disk, in particular in locations we associate with γ -ray radiation from the dilute ISM.

A better understanding of the astrophysical γ -ray radiation is therefore necessary to confirm or refute the apparent DM annihilation signal. Our current sensitivity is more limited by astrophysical modeling uncertainties than by the photon count statistics. The phenomenological and morphological investigations presented here, as well as the physical modeling approaches by other groups, need to be refined to deal with the large spatial and spectral complexity of the real Galactic γ -ray emission.

Acknowledgements

We gratefully thank Simon D. M. White, Christoph Weniger, and an anonymous referee for feedback and comments on the manuscript. X. H. thanks Alejandro Ibarra for useful discussions and suggestions. T. E. and X. H. thank Andreas Müller and the *European Centre for Theoretical Studies in Nuclear Physics and Related Areas* in Trento for the stimulating workshop atmosphere, which encouraged this research. This research was supported by the DFG cluster of excellence Origin and Structure of the Universe (www.universe-cluster.de).

References

- [1] F. Zwicky, *Die Rotverschiebung von extragalaktischen Nebeln*, *Helv. Phys. Acta* **6** (1933) 110–127.
- [2] G. Jungman, M. Kamionkowski, and K. Griest, *Supersymmetric dark matter*, *Phys.Rept.* **267** (1996) 195–373, [[hep-ph/9506380](https://arxiv.org/abs/hep-ph/9506380)].
- [3] G. Bertone, D. Hooper, and J. Silk, *Particle dark matter: Evidence, candidates and constraints*, *Phys.Rept.* **405** (2005) 279–390, [[hep-ph/0404175](https://arxiv.org/abs/hep-ph/0404175)].

- [4] **Planck** Collaboration, P. Ade *et. al.*, *Planck 2013 results. XVI. Cosmological parameters*, [arXiv:1303.5076](#).
- [5] **PAMELA** Collaboration, O. Adriani *et. al.*, *An anomalous positron abundance in cosmic rays with energies 1.5-100 GeV*, *Nature* **458** (2009) 607–609, [[arXiv:0810.4995](#)].
- [6] **AMS** Collaboration, M. Aguilar *et. al.*, *First Result from the Alpha Magnetic Spectrometer on the International Space Station: Precision Measurement of the Positron Fraction in Primary Cosmic Rays of 0.5C350 GeV*, *Phys.Rev.Lett.* **110** (2013) 141102.
- [7] **PAMELA** Collaboration, O. Adriani *et. al.*, *The cosmic-ray electron flux measured by the PAMELA experiment between 1 and 625 GeV*, *Phys.Rev.Lett.* **106** (2011) 201101, [[arXiv:1103.2880](#)].
- [8] J. Chang, J. Adams, H. Ahn, G. Bashindzhagyan, M. Christl, *et. al.*, *An excess of cosmic ray electrons at energies of 300-800 GeV*, *Nature* **456** (2008) 362–365.
- [9] **Fermi LAT** Collaboration, M. Ackermann *et. al.*, *Measurement of separate cosmic-ray electron and positron spectra with the Fermi Large Area Telescope*, *Phys.Rev.Lett.* **108** (2012) 011103, [[arXiv:1109.0521](#)].
- [10] W. Atwood, R. Bagagli, L. Baldini, R. Bellazzini, G. Barbiellini, *et. al.*, *Design and Initial Tests of the Tracker-Converter of the Gamma-ray Large Area Space Telescope*, *Astropart.Phys.* **28** (2007) 422–434.
- [11] **Fermi-LAT** Collaboration, W. Atwood *et. al.*, *The Large Area Telescope on the Fermi Gamma-ray Space Telescope Mission*, *Astrophys.J.* **697** (2009) 1071–1102, [[arXiv:0902.1089](#)].
- [12] T. Bringmann, X. Huang, A. Ibarra, S. Vogl, and C. Weniger, *Fermi LAT Search for Internal Bremsstrahlung Signatures from Dark Matter Annihilation*, *JCAP* **1207** (2012) 054, [[arXiv:1203.1312](#)].
- [13] C. Weniger, *A Tentative Gamma-Ray Line from Dark Matter Annihilation at the Fermi Large Area Telescope*, *JCAP* **1208** (2012) 007, [[arXiv:1204.2797](#)].
- [14] **Fermi-LAT** Collaboration, M. Ackermann *et. al.*, *Search for Gamma-ray Spectral Lines with the Fermi Large Area Telescope and Dark Matter Implications*, *Phys.Rev.* **D88** (2013) 082002, [[arXiv:1305.5597](#)].
- [15] **Fermi-LAT** Collaboration, M. Ackermann *et. al.*, *Updated search for spectral lines from Galactic dark matter interactions with pass 8 data from the Fermi Large Area Telescope*, *Phys. Rev.* **D91** (2015), no. 12 122002, [[arXiv:1506.0001](#)].
- [16] A. Ibarra, A. S. Lamperstorfer, S. L. Gehler, M. Pato, and G. Bertone, *On the sensitivity of CTA to gamma-ray boxes from multi-TeV dark matter*, [arXiv:1503.0679](#).
- [17] X. Huang *et. al.*, *Perspective of monochromatic gamma-ray line detection with the High Energy cosmic-Radiation Detection (HERD) facility onboard China’s Space Station*, [arXiv:1509.0267](#).
- [18] C. van Eldik, *Gamma rays from the Galactic Centre region: a review*, *Astropart. Phys.* **71** (2015) 45–70, [[arXiv:1505.0605](#)].
- [19] L. Goodenough and D. Hooper, *Possible Evidence For Dark Matter Annihilation In The Inner Milky Way From The Fermi Gamma Ray Space Telescope*, [arXiv:0910.2998](#).
- [20] **Fermi-LAT** Collaboration, V. Vitale and A. Morselli, *Indirect Search for Dark Matter from the center of the Milky Way with the Fermi-Large Area Telescope*, [arXiv:0912.3828](#).
- [21] D. Hooper and L. Goodenough, *Dark Matter Annihilation in The Galactic Center As Seen by the Fermi Gamma Ray Space Telescope*, *Phys.Lett.* **B697** (2011) 412–428, [[arXiv:1010.2752](#)].
- [22] D. Hooper and T. Linden, *Gamma Rays From The Galactic Center and the WMAP Haze*, *Phys.Rev.* **D83** (2011) 083517, [[arXiv:1011.4520](#)].

- [23] K. N. Abazajian and M. Kaplinghat, *Detection of a Gamma-Ray Source in the Galactic Center Consistent with Extended Emission from Dark Matter Annihilation and Concentrated Astrophysical Emission*, *Phys.Rev.* **D86** (2012) 083511, [[arXiv:1207.6047](#)].
- [24] C. Gordon and O. Macias, *Dark Matter and Pulsar Model Constraints from Galactic Center Fermi-LAT Gamma Ray Observations*, *Phys.Rev.* **D88** (2013) 083521, [[arXiv:1306.5725](#)].
- [25] W.-C. Huang, A. Urbano, and W. Xue, *Fermi Bubbles under Dark Matter Scrutiny. Part I: Astrophysical Analysis*, [arXiv:1307.6862](#).
- [26] D. Hooper and T. R. Slatyer, *Two Emission Mechanisms in the Fermi Bubbles: A Possible Signal of Annihilating Dark Matter*, *Phys.Dark Univ.* **2** (2013) 118–138, [[arXiv:1302.6589](#)].
- [27] T. Daylan, D. P. Finkbeiner, D. Hooper, T. Linden, S. K. N. Portillo, *et. al.*, *The Characterization of the Gamma-Ray Signal from the Central Milky Way: A Compelling Case for Annihilating Dark Matter*, [arXiv:1402.6703](#).
- [28] F. Calore, I. Cholis, and C. Weniger, *Background model systematics for the Fermi GeV excess*, *JCAP* **1503** (2015) 038, [[arXiv:1409.0042](#)].
- [29] P. Agrawal, B. Batell, P. J. Fox, and R. Harnik, *WIMPs at the Galactic Center*, *JCAP* **1505** (2015) 011, [[arXiv:1411.2592](#)].
- [30] J. F. Navarro, C. S. Frenk, and S. D. White, *The Structure of cold dark matter halos*, *Astrophys.J.* **462** (1996) 563–575, [[astro-ph/9508025](#)].
- [31] J. F. Navarro, C. S. Frenk, and S. D. White, *A Universal density profile from hierarchical clustering*, *Astrophys.J.* **490** (1997) 493–508, [[astro-ph/9611107](#)].
- [32] B. Zhou, Y.-F. Liang, X. Huang, X. Li, Y.-Z. Fan, L. Feng, and J. Chang, *GeV excess in the Milky Way: The role of diffuse galactic gamma-ray emission templates*, *Phys. Rev.* **D91** (2015), no. 12 123010, [[arXiv:1406.6948](#)].
- [33] N. Mirabal, *Dark matter vs. Pulsars: Catching the impostor*, *Mon.Not.Roy.Astron.Soc.* **436** (2013) 2461, [[arXiv:1309.3428](#)].
- [34] Q. Yuan and B. Zhang, *Millisecond pulsar interpretation of the Galactic center gamma-ray excess*, [arXiv:1404.2318](#).
- [35] F. Calore, M. Di Mauro, and F. Donato, *Diffuse gamma-ray emission from galactic Millisecond Pulsars*, [arXiv:1406.2706](#).
- [36] D. Hooper, I. Cholis, T. Linden, J. Siegal-Gaskins, and T. Slatyer, *Pulsars Cannot Account for the Inner Galaxy’s GeV Excess*, *Phys. Rev.* **D88** (2013) 083009, [[arXiv:1305.0830](#)].
- [37] I. Cholis, D. Hooper, and T. Linden, *Challenges in Explaining the Galactic Center Gamma-Ray Excess with Millisecond Pulsars*, *JCAP* **1506** (2015), no. 06 043, [[arXiv:1407.5625](#)].
- [38] J. Petrovic, P. D. Serpico, and G. Zaharijas, *Millisecond pulsars and the Galactic Center gamma-ray excess: the importance of luminosity function and secondary emission*, *JCAP* **1502** (2015), no. 02 023, [[arXiv:1411.2980](#)].
- [39] S. K. Lee, M. Lisanti, B. R. Safdi, T. R. Slatyer, and W. Xue, *Evidence for Unresolved Gamma-Ray Point Sources in the Inner Galaxy*, *ArXiv e-prints* (June, 2015) [[arXiv:1506.0512](#)].
- [40] R. Bartels, S. Krishnamurthy, and C. Weniger, *Strong support for the millisecond pulsar origin of the Galactic center GeV excess*, *ArXiv e-prints* (June, 2015) [[arXiv:1506.0510](#)].
- [41] M. Selig, V. Vacca, N. Oppermann, and T. A. Enlin, *The denoised, deconvolved, and decomposed Fermi γ -ray sky - An application of the D³PO algorithm*, *Astron. Astrophys.* **581** (2015) A126, [[arXiv:1410.4562](#)].
- [42] M. Selig and T. A. Enßlin, *Denoising, deconvolving, and decomposing photon observations*.

- derivation of the d^3p_0 algorithm, *Astron. Astrophys.* **574** (Feb., 2015) A74, [[arXiv:1311.1888](#)].
- [43] T. A. Ensslin, M. Frommert, and F. S. Kitaura, *Information field theory for cosmological perturbation reconstruction and non-linear signal analysis*, *Phys. Rev.* **D80** (2009) 105005, [[arXiv:0806.3474](#)].
- [44] M. Selig, M. R. Bell, H. Junklewitz, N. Oppermann, M. Reinecke, M. Greiner, C. Pachajoa, and T. A. Ensslin, *NIFTY - Numerical Information Field Theory - a versatile Python library for signal inference*, *Astron. Astrophys.* **581** (2013) A26, [[arXiv:1301.4499](#)].
- [45] G. Dobler, D. P. Finkbeiner, I. Cholis, T. R. Slatyer, and N. Weiner, *The Fermi Haze: A Gamma-Ray Counterpart to the Microwave Haze*, *Astrophys. J.* **717** (2010) 825–842, [[arXiv:0910.4583](#)].
- [46] M. Su, T. R. Slatyer, and D. P. Finkbeiner, *Giant Gamma-ray Bubbles from Fermi-LAT: AGN Activity or Bipolar Galactic Wind?*, *Astrophys. J.* **724** (2010) 1044–1082, [[arXiv:1005.5480](#)].
- [47] **Fermi-LAT** Collaboration, M. Ackermann *et. al.*, *The Spectrum and Morphology of the Fermi Bubbles*, *Astrophys. J.* **793** (2014), no. 1 64, [[arXiv:1407.7905](#)].
- [48] **Planck** Collaboration, A. Abergel *et. al.*, *Planck 2013 results. XI. All-sky model of thermal dust emission*, *Astron. Astrophys.* **571** (2014) A11, [[arXiv:1312.1300](#)].
- [49] D. P. Finkbeiner, M. Davis, and D. J. Schlegel, *Extrapolation of galactic dust emission at 100 microns to CMBR frequencies using FIRAS*, *Astrophys. J.* **524** (1999) 867–886, [[astro-ph/9905128](#)].
- [50] E. Carretti, R. M. Crocker, L. Staveley-Smith, M. Haverkorn, C. Purcell, B. M. Gaensler, G. Bernardi, M. J. Kesteven, and S. Poppi, *Giant Magnetized Outflows from the Centre of the Milky Way*, *Nature* **493** (2013) 66, [[arXiv:1301.0512](#)].
- [51] R. Catena and P. Ullio, *A novel determination of the local dark matter density*, *JCAP* **1008** (2010) 004, [[arXiv:0907.0018](#)].
- [52] P. Salucci, F. Nesti, G. Gentile, and C. F. Martins, *The dark matter density at the Sun's location*, *Astron. Astrophys.* **523** (2010) A83, [[arXiv:1003.3101](#)].
- [53] F. Iocco, M. Pato, G. Bertone, and P. Jetzer, *Dark Matter distribution in the Milky Way: microlensing and dynamical constraints*, *JCAP* **1111** (2011) 029, [[arXiv:1107.5810](#)].
- [54] M. Cirelli, G. Corcella, A. Hektor, G. Hutsi, M. Kadastik, P. Panci, M. Raidal, F. Sala, and A. Strumia, *PPPC 4 DM ID: A Poor Particle Physicist Cookbook for Dark Matter Indirect Detection*, *JCAP* **1103** (2011) 051, [[arXiv:1012.4515](#)]. [Erratum: *JCAP*1210,E01(2012)].
- [55] R.-z. Yang and F. Aharonian, *On the "GeV excess" in the diffuse γ -ray emission towards the Galactic Center*, [arXiv:1602.0676](#).
- [56] E. Carlson, T. Linden, and S. Profumo, *Improved Cosmic-Ray Injection Models and the Galactic Center Gamma-Ray Excess*, [arXiv:1603.0658](#).
- [57] J. Petrovic, P. D. Serpico, and G. Zaharijas, *Galactic Center gamma-ray "excess" from an active past of the Galactic Centre?*, *JCAP* **1410** (2014), no. 10 052, [[arXiv:1405.7928](#)].
- [58] I. Cholis, C. Evoli, F. Calore, T. Linden, C. Weniger, and D. Hooper, *The Galactic Center GeV Excess from a Series of Leptonic Cosmic-Ray Outbursts*, [arXiv:1506.0511](#).
- [59] D. Gaggero, M. Taoso, A. Urbano, M. Valli, and P. Ullio, *Towards a realistic astrophysical interpretation of the Galactic center excess*, [arXiv:1507.0612](#).
- [60] T. Bringmann, F. Calore, M. Di Mauro, and F. Donato, *Constraining dark matter annihilation with the isotropic γ -ray background: updated limits and future potential*, *Phys. Rev.* **D89** (2014), no. 2 023012, [[arXiv:1303.3284](#)].
- [61] I. Cholis, D. Hooper, and S. D. McDermott, *Dissecting the Gamma-Ray Background in Search*

- of Dark Matter*, *JCAP* **1402** (2014) 014, [[arXiv:1312.0608](#)].
- [62] M. Di Mauro and F. Donato, *Composition of the Fermi-LAT isotropic gamma-ray background intensity: Emission from extragalactic point sources and dark matter annihilations*, *Phys. Rev. D* **91** (2015), no. 12 123001, [[arXiv:1501.0531](#)].
- [63] M. Fornasa and M. A. Sanchez-Conde, *The nature of the Diffuse Gamma-Ray Background*, *Phys. Rept.* **598** (2015) 1–58, [[arXiv:1502.0286](#)].
- [64] **Fermi-LAT** Collaboration, M. Ackermann *et. al.*, *The spectrum of isotropic diffuse gamma-ray emission between 100 MeV and 820 GeV*, *Astrophys. J.* **799** (2015) 86, [[arXiv:1410.3696](#)].